Performance Evaluation of Scheduling in 5G-mmWave Networks under Human Blockage

Fadhil Firyaguna, Andrea Bonfante, Jacek Kibiłda and Nicola Marchetti

***Abstract*—The millimetre-wave spectrum provisions enormous enhancement to the achievable data rate of 5G networks. However, human blockages affecting the millimetre-wave signal can severely degrade the performance if proper resource allocation is not considered. In this paper, we assess how conventional schedulers, such as the Proportional Fair scheduler, react to the presence of blockage. Our results show that the resource allocation may disfavour users suffering from blockage, leading to low data rate for those users. To circumvent this problem, we show that the data rate of those users can be improved by using a scheduler adapted to react to upcoming blockage events. The adapted scheduler aims at proactively allocating the resources before a blockage happens, mitigating losses. Such adaptation is motivated by recent progress in blockage prediction for millimetre-wave signals in a dynamic human blockage scenario. Our extensive simulations indicate gains in the 1st percentile rate and fairness with respect to Proportional Fair scheduler when blockage conditions are severe.**

***Index Terms*—5G, mmWave, blockage, resource allocation, scheduling.**

I. Introduction

The millimetre-wave (mmWave) spectrum is key to enhance the capacity of the fifth-generation (5G) of cellular networks and support multi-Gbps applications. However, transmission in mmWave frequencies may be severely affected by obstructions, such as human bodies. The blockage caused by a human body may add as much as 40 dB of attenuation to the mmWave signal [1], which can lead to radio link failures. Human blockages can be frequent in crowded places such as transportation hubs and sport arenas. This frequent, and potentially abrupt, disruption to the signal quality may impact the effectiveness of radio resource scheduling algorithms.

Blockage-aware scheduling algorithms have been adopted in the context of mmWaves for relay-assisted networks, where the blockage problem is handled through allocating the transmissions over multi-hop relay paths and thus preventing possible disruptions and enabling seamless connectivity [2]. However, there is a lack of studies in the context of networks where relay nodes or other access points (APs) are not available for re-connection in the event of a blockage. In this context, a user equipment (UE) suffering from frequent blockage can have its transmission rate severely reduced, increasing the discrepancy to other UEs operating in favourable channel conditions, as we will also show in our numerical evaluation.

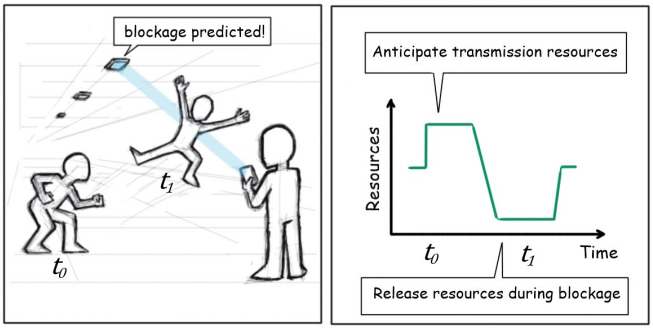

Fig. 1: Preemptive resource allocation for users that might be blocked.

In this paper, we evaluate the performance of resource allocation algorithms, based on the conventional Proportional Fair (PF) scheduler, in the presence of mmWave signal blockages. We consider that the resource allocation is performed to multiple users, each of which may experience abrupt disruptions to signal quality caused by the human body blockage. Since the PF scheduler prioritises the allocation based on the achievable transmission rate, UEs suffering from blockage may have the feasible rate degraded and thus be given progressively lower priority, disfavouring the assignment to those UEs. Hence, the challenge is to adapt the scheduler in such way that the allocation considers these signal disruptions and possible rate degradation in the following moments, and thus produces more fair assignment to UEs suffering from blockage.

With the development of blockage prediction mechanisms, a scheduler may effectively mitigate the blockage effects, as we will show in this work. Blockage prediction in mmWave communications can be performed by: (i) inferring the mmWave channel from the sub-6 GHz channel observation [3], [4], (ii) observing the past mmWave beamforming vectors [5], [6] or (iii) using camera images to track the movement of potential obstructions [7], [8]. Those methods can produce blockage indicators that will help the system predict the channel status. The scheduler can use these methods to anticipate transmission to a user that might be blocked and preemptively allocate resources, as illustrated in Fig. 1.

A. Related Works

Prediction-based schedulers have been studied in the context of previous generations of wireless systems [9]–[12]. These schedulers rely on predicted and measured information that includes fading channel gains, mobility pattern (predicted

The authors are with CONNECT Centre, Trinity College Dublin, Ireland. E-mail: {firyaguf, bonfanta, kibildj, nicola.marchetti}@tcd.ie.

This publication has emanated from the research conducted within the scope of *NEMO (Enabling Cellular Networks to Exploit Millimeter-wave Opportunities)* project financially supported by the Science Foundation Ireland (SFI) under Grant No. 14/US/I3110 and with partial support of the European Regional Development Fund under Grant No. 13/RC/2077.

route of a user through a region) and radio coverage map (mapping between measured signal strengths and geographical locations). The prediction of the fading channel in the upcoming transmission intervals allowed these schedulers to estimate the achievable rates with increased precision, improving the network performance under the effects of rapid fluctuations of the received signal strength due to fast-fading at sub-6 GHz frequencies. However, as the accuracy of fading prediction can degrade rapidly with the prediction horizon (few milliseconds, depending on the mobility scenario) [11], the schedulers proposed in [9]–[11], [13] have to update their prediction and re-optimise scheduling every millisecond. When considering mobility, the scheduler in [12] uses the prediction of the mobility pattern together with the radio coverage map to estimate the achievable rate and allocate resources accordingly. It was shown that this approach can significantly improve network performance for urban mobility scenarios and slow-fading channels. However, none of these works, e.g., [9]–[12], account for the effect of the mmWave channel propagation characteristics, including the blockage effect.

For 5G wireless systems, most of the works have been focusing on developing schedulers to improve the fairness in heterogeneous networks [14] and the cell edge throughput [15]. Still, they do not consider the blockage effects on the channel and on the scheduler design. Therefore, it is not clear how those schedulers will react to blockages. In such conditions, the channel quality of a user can be more affected than, or as much as, the channel of cell edge users in 5G-mmWave networks.

On the other hand, blockage-aware schedulers have been adopted for relay-assisted networks (WPAN, WLAN, 5G wireless backhaul) [2], [16]–[21], where the scheduling algorithm can allocate a transmission to a relay AP when the UE link to the serving AP becomes blocked. Such scheduling algorithms make their decision after a blockage event (reactive scheduling) and may have to re-calculate the decision every time a blockage occurs, potentially increasing overhead as blockage frequency increases.

B. Contributions

In contrast to the reactive methods proposed in [2], [16]–[21], our work considers that the scheduler could instead have a proactive approach with the aid of prediction mechanisms. Since human blockage represents a significant challenge for the 5G systems design, new prediction methods have been recently studied in [4], where one proposes the utilisation of sub-6 GHz signal to provide an early warning of blockage in the mmWave signal, and in [3], [5], [7], [8], [22] where one proposes to use camera images to construct a prediction model from a dataset of sequential images involving the geometry and mobility of obstacles and labelled with the received power. Using such methods, blockages can be forecasted up to tens of milliseconds ahead, giving the system sufficient time to adapt. These positive blockage prediction results motivate us to revisit scheduler design for mmWave networks. In our work, we assume there exists a prediction mechanism, such as the one proposed in [7] that allows the system to predict the received power in a given time window and to estimate future data rates based on that prediction. The early-warning blockage indicator allows the scheduler to have sufficient time to allocate resources in order to mitigate the losses in performance caused by the transition from line-of-sight (LOS) to blocked state. With this system, we can implement a scheduler that allocates resources in future transmission intervals according to the estimated data rates and test its performance against the conventional schedulers.

Secondly, as the main objective of the allocation techniques proposed in [4]–[8], [22]–[26] is to select a different path to avoid blockage, in our work we study an alternative way to mitigate blockage effects when there is no other cell to hand-off to. Indeed, our work aims to evaluate how the conventional resource allocation methods behave under blockage when there is no spatial macro-diversity (single AP), and to study how they can be adapted to cope better with the blockage effects.

In summary, the main contributions of this work account for:

- We show that users suffering from blockage are disfavoured in the resource allocation because conventional schedulers do not react quickly enough in case of blockage. This result shows that conventional schedulers, to be applied in 5G and beyond networks, should be adapted to cope with the impairments of the mmWave propagation.
- We show that an adaptation of the PF scheduler can be made by changing the priority metric to consider the blockage prediction. We refer to this adapted scheduler as the Blockage-Aware Predictive Proportional Fair (BA-PF) scheduler. We also show that using BA-PF it is possible to increase resource allocation before the channel quality drops and reduce the allocation thereafter.

The rest of the paper is organised as follows: we describe our system model in Section II, we evaluate the user data rate performance, comparing our BA-PF scheduler to conventional schedulers in Section III and we summarise our findings in Section IV.

II. System Model

A. Frame Structure

We study the downlink transmission of a single ceiling-mounted indoor mmWave AP which transmits to n_U UEs using orthogonal frequency-division multiple access (OFDMA) during T ms. Data transmission occurs in time-slots with duration Δ_t and in a bandwidth b divided in n_{SC} sub-carriers. At the medium access control (MAC) layer, we assume a scheduler assigns all sub-carriers at a time-slot t to a UE having index $u \in \{1, \ldots, n_U\}$. This assignment is represented by a vector $\mathbf{X}$, with size $T/\Delta t$ elements, defined for each UE. When the time-slot t is assigned to UE u, the scheduler sets $x_u(t) = 1$. Otherwise, the scheduler sets $x_u(t) = 0$.

B. Channel Model

The LOS path between AP and UE can be obstructed by blockage, such as a moving pedestrian or the user body itself, which can decrease the received signal power. We assume

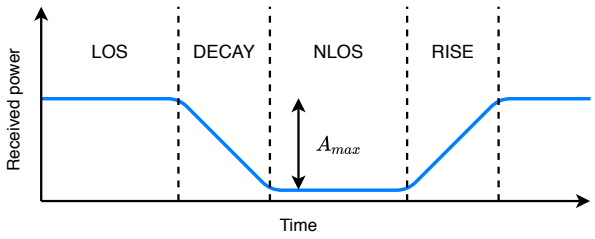

Fig. 2: Four-state blockage model.

the blockage event is modelled according to the four-state model described in [1] and affects the channel quality of the whole link bandwidth for each UE independently. We denote as $s \in \{\text{LOS}, \text{NLOS}, \text{DECAY}, \text{RISE}\}$ the states of the AP-UE link and we represent them in Fig. 2. The LOS state denotes the link having LOS propagation conditions, while the NLOS state denotes the link being obstructed by blockage. Moreover, the DECAY state denotes the transition state from LOS to NLOS and is characterised by a decay factor ρ_{D} dB/s. The RISE state denotes the transition state from NLOS to LOS and is characterised by a factor ρ_{R} dB/s.

We assume that the blockers' arrivals follow a Poisson process with average arrival rate λ_{B} blockers/s, and the blockage state has duration which is exponentially distributed with average value τ_{B} ms [27]. The blockage attenuation power $A(t)$ varies according to the channel state and can be expressed as

$$A(t) = \begin{cases} 0 & \text{if } s\text{=LOS}, \\ \rho_{\text{D}} \cdot (t - t_{\text{D}}) & \text{if } s\text{=DECAY}, \\ A_{\text{max}} & \text{if } s\text{=NLOS}, \\ A_{\text{max}} - \rho_{\text{R}} \cdot (t - t_{\text{R}}) & \text{if } s\text{=RISE}, \end{cases} \tag{1}$$

where t_{D} and t_{R} represent the time instants when the states DECAY and RISE start. We also assume that if multiple blockers arrive together, the channel remains in NLOS state for the duration of the longest blockage event.

The link budget for the channel between AP and UE u in the time-slot t can expressed as,

$$p_{\text{rx,u}}(t) = p_{\text{tx}} \cdot g_{\text{tx}} \cdot g_{\text{rx}} \cdot \ell_0 \cdot d_u^{-\nu} \cdot A(t), \tag{2}$$

where p_{tx} is the transmit power, g_{tx} is the transmit antenna gain, g_{rx} is the receive antenna gain, ℓ_0 is the path loss at one metre distance under free space propagation conditions, d_u is the AP-UE distance and ν is the attenuation exponent.

We define the signal-to-noise ratio (SNR) as:

$$z_u(t) = \frac{p_{\text{rx,u}}(t)}{p_{\text{n}}}, \tag{3}$$

where p_{n} represents the noise power over bandwidth b. The instantaneous user data rate can be expressed as:

$$r_u(t) = b \cdot \log_2(1 + z_u(t)) \cdot x_u(t) \cdot \mathbb{1}(z_u(t) > \zeta), \tag{4}$$

where $\mathbb{1}(\cdot)$ is a binary function that indicates when the link goes to outage, i.e. $z_u(t) < \zeta$, and the data rate becomes $r_u(t) = 0$.

C. Conventional Scheduling Algorithms

The conventional PF scheduler aims to provide a fair distribution of resources among the set of UEs that are served by the AP. Within the pool of UEs to schedule there can be UEs experiencing favourable channel conditions and UEs with less favourable channel conditions. To obtain a fair allocation, the PF scheduler gives priority to the UEs that have the highest ratio between the feasible rate at the current time-slot and the average rate over former successive time-slots [28], [29]. The PF scheduler policy to assign the user u^* in the time-slot t can be expressed as

$$u^* = \arg\max_u \frac{r_u(t)}{\bar{r}_u(t-1)}, \tag{5}$$

where $\bar{r}_u(t)$ is the average rate of user u in the time slot t, and is calculated based on an exponential moving average:

$$\bar{r}_u(t) = (1 - w)\, \bar{r}_u(t-1) + w\, r_u(t), \tag{6}$$

where $w \in [0, 1]$ is a system parameter that weights the importance of the current feasible rate with respect to the average rate when computing the average rate metric.

On the other hand, the Maximise Minimum Rate (MaxMin) scheduler aims to maximise the minimum rate of the UEs. This is done by prioritising the UE with the lowest average rate. The MaxMin scheduler policy to assign the user u^* in the time-slot t can be expressed as

$$u^* = \arg\max_u \frac{1}{\bar{r}_u(t-1)}. \tag{7}$$

Under the effect of blockage, the policies described in Equations (5) and (7) may lead to a decrease of the UE average rate. This effect results from the detrimental impact of the blockage attenuation on the feasible data rate. In detail, the above scheduling policies' specific behaviours can be described as follows:

- The PF priority function in (5) is directly proportional to the current feasible rate. Thus, as the feasible rate decreases with blockage attenuation, the priority of UEs suffering from blockage decreases, giving more priority to UEs in favourable conditions. This decrease in the priority is not immediate since the priority is also inversely proportional to the average rate that decreases slower than the feasible rate, depending on the weight of the moving average.
- The MaxMin priority function in (7) is inversely proportional to the average rate. It means that, even when the UE is in outage, the priority keeps increasing from slot to slot as the average rate decreases. Thus, more slots are allocated to the UE suffering from blockage and fewer slots to UEs in favourable conditions.

Therefore, both the PF and MaxMin schedulers suffer in case of blockage. In the first case, only a few slots are allocated by the PF scheduler when it is most needed, while in the second case too many slots are allocated by the MaxMin scheduler when they are not needed.

D. Blockage-Aware Proportional Fair Scheduling in mmWave Spectrum

To circumvent the scheduling inefficiencies caused by the blockage effect, we study the use of a predictive scheduler that leverages the estimation of the channel status in future slots similarly to the ones proposed in [9]–[11], [13]. Differently from [9]–[11], [13], we study the application to the mmWave network use case, where it is potentially possible to predict the received power degradation due to temporary link blockage [7]. Therefore, we assume that the system can predict the received power n_T slots in advance, where n_T is the prediction window. We model the potential error due to inaccurate predictions with a random variable $E \sim \mathcal{N}(0, \sigma^2)$ [10], [30] which is added to the future ground-truth values of the received power obtained from simulations to model the predicted received power $\hat{p}_{\text{rx,u}}(t)$. We also assume that σ increases with the prediction window size given that the prediction accuracy decreases [7].

Hence, the estimated signal-to-noise ratio (SNR) $\hat{z}_u(t')$ at a future time-slot $t' < t + n_T$ can be expressed as:

$$\hat{z}_u(t') = \frac{p_{\text{rx,u}}(t') + E}{p_{\text{n}}}. \tag{8}$$

We assume that a blockage is detected by the predictor when the estimated received power $\hat{p}_{\text{rx,u}}(t')$ shows significant variations within the prediction window. Conversely, we assume that there is no blockage when $\hat{p}_{\text{rx,u}}(t')$ remains constant over time.[1]

Once a blockage is predicted, and given the estimated channel quality, a predictive scheduler will allocate more resources to those UEs which are to suffer from the blockage. In practice, the UE priority is modified expressing the denominator of the BA-PF scheduler policy as a sum of the predicted feasible rates at future time-slots. For the future time-slots at the end of the prediction window, the predicted rate for the blocked UEs is expected to be low due to the blockage attenuation, making the denominator smaller than it would have been for if the UEs had not been affected by the blockage. Consequently, the UEs predicted as blocked are assigned a higher priority than the other UEs and are likely to be granted more scheduling opportunities for the future time-slots at the beginning of the prediction window. For those time-slots, their channels still experience favourable propagation conditions. On the other hand, the UEs which are predicted as non-blocked may have more scheduling opportunities in the last slots of the prediction window, when the channels of the blocked UE will be affected by a strong blockage attenuation and are assigned a low priority which allows to release the resources to those non-blocked UEs.

Hence, we adapt the priority function in (5) to make the PF scheduler blockage-aware (BA-PF). The BA-PF scheduler policy to assign the user u^* in the time-slot t' can be expressed as

$$u^* = \arg\max_u \frac{\hat{r}_u(t')}{S_u(t')}, \tag{9}$$

[1]As the main focus of our work is to evaluate the scheduling performance under blockage effect, we assume that in this type of scenario the attenuation due to the blockers over time prevails on other time-dependent components such as fast fading or interference.

where $\hat{r}_u(t')$ is the feasible instantaneous user rate at a future time-slot $t' \in [t+1, t+n_T]$ and can be computed as:

$$\hat{r}_u(t') = b \cdot \log_2(1 + \hat{z}_u(t')) \cdot \mathbb{1}(\hat{z}_u(t') > \zeta). \tag{10}$$

and $S_u(t')$ is the estimated sum-rate of all time-slots from t' to $t+n_{\text{T}}$ given the allocation vector $\mathbf{X}_u$ and can be expressed as:

$$S_u(t') = \sum_{j=t'}^{t+n_{\text{T}}} \hat{r}_u(j) \cdot x_u(j). \tag{11}$$

Thus, the assignment of the first slots depends on how the following slots in the future are assigned. Because of that, the time-slot assignment starts from the end of the prediction window at time-slot $t' = t+n_{\text{T}}$ and works backwards to time-slot $t' = t+1$, as shown in Algorithm 1.

Algorithm 1: BA-PF scheduling algorithm

Result: Allocation assignment x
$x_u(t') = 0, \quad \forall\, u, t'$;
if *blockage is predicted to happen during any of the next* n_T *slots* **then**
  for $t' = t + n_T$ *down to* t **do**
    for $u = 1$ *to* n_U **do**
      $S_u(t') = \sum_{j=t'}^{t+n_{\text{T}}} \hat{r}_u(j) \cdot x_u(j)$;
    end
    $u^* = \arg\max_u \frac{r_u(t')}{S_u(t')}$;
    $x_{u*}(t') = 1$;
  end
else
  Execute PF algorithm.
end

For instance, consider a UE u that suffers from blockage and has the estimated rate ($\hat{r}_u$) degraded in the future. Because of the backward iteration, other UEs were allocated in the last slots as $\hat{r}_u$ is lower than the estimated rates of the other UEs. Hence, as the iteration reaches the first slots, $\hat{r}_u$ is high and S_u is low since very few time-slots have been allocated to UE u, leading to a increased priority function according to (9). Therefore UE u has the transmission anticipated as it gets more priority in the first slots and releases the last slots for UEs with better channel conditions.

III. Numerical Results

A. Simulation Setup

In this section, we evaluate and compare the PF, MaxMin and BA-PF schedulers performance. As depicted in Fig. 3, we consider a single ceiling-mounted AP that is positioned in the centre of the network area at a height of 2 m above the UE antennas and is equipped with a directive antenna facing downward having beamwidth 170 ° and gain of 3.16 dBi [31]. The UEs are uniformly distributed in the AP coverage area (of radius ρ =15 m), are equipped with an omnidirectional receiver antenna and are all served from the same AP.

The channel model parameters are in line with empirically-tested model described in [32] having LOS channel state with parameters $\ell_0 = 63.4\,\text{dB}$ and $\nu = 1.72$. We assume maximum blockage attenuation $A_{\max} = 40\,\text{dB}$, decay rate $\rho_{\text{D}} = 0.2\,\text{dB/ms}$, and rise rate $\rho_{\text{R}} = 6.7\,\text{dB/ms}$, in line with the measurements reported in [33].

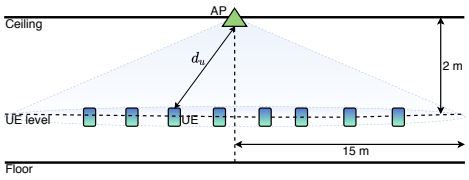

Fig. 3: Ceiling-mounted AP setup with downward facing beam illuminating the UEs.

We simulate a sequence of 48000 time-slots of an OFDMA frame transmission with carrier frequency of 60 GHz according to the 5G new radio (NR) standard [34]. We gain insights on the various schedulers by changing the characteristics of the blockage scenario, including different blockers' arrival rate λ_{B} and blockage duration τ_{B}. To analyse the impact of the blockage effects on scheduling, we evaluate the empirical cumulative distribution function (ECDF) of the average user data rate. The 1st percentile rate, mean rate and fairness metrics are selected for performance evaluation. The 1st percentile rate can be interpreted as the average data rate of the UEs that are most affected by blockage. The mean rate is defined as the sum of the average user rates divided by the number of UEs in the cell, and fairness is defined as the Jain's fairness index [35]. Settings for the system parameters are provided in Table I.

TABLE I: System parameters

Number of UEs	n_U	8
Slot duration	Δt	62.5 μs
Frame bandwidth	b	2 GHz
Moving average weight	w	0.5
Transmit power	p_{tx}	100 mW
Noise figure		9 dB
Noise power	p_n	-71.99 dBm
SNR threshold	ζ	0 dB
AP beamwidth		170 °
AP antenna gain	g_{tx}	3.16 dBi
UE antenna gain	g_{rx}	0 dBi
Prediction window	n_T	{50, 200, 500} ms
Prediction error	σ	{ 10^{-3},10^{-2},10^{-1}}

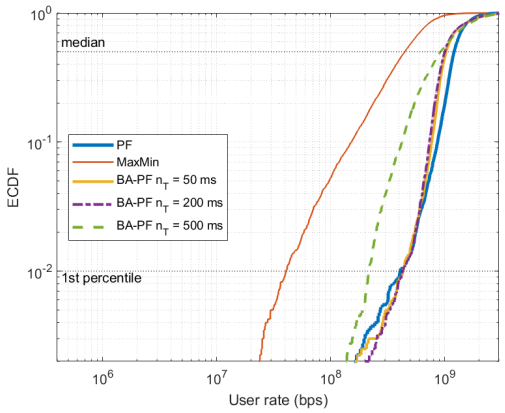

(a) $\lambda_{\text{B}} = 0.2$ blockers/s, $\tau_{\text{B}} = 1000$ ms

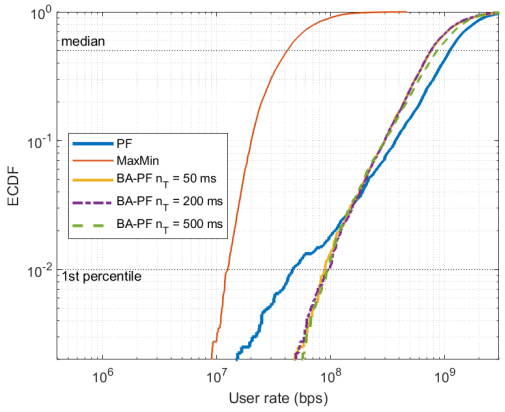

(b) $\lambda_{\text{B}} = 1.0$ blockers/s, $\tau_{\text{B}} = 1000$ ms

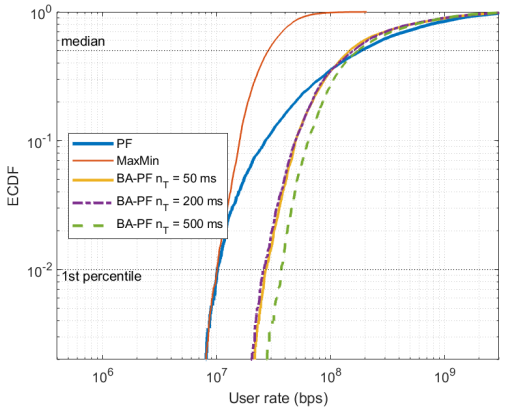

(c) $\lambda_{\text{B}} = 2.0$ blockers/s, $\tau_{\text{B}} = 3000$ ms

Fig. 4: Empirical cumulative distribution function of the user rate for different blockage scenarios with eight UEs in the cell.

B. User Performance

In Fig. 4 we show the ECDFs of the average user rate for the PF, MaxMin and BA-PF schedulers in three different blockage scenarios: (a) low blockers' arrival rate, short blockage duration (Fig. 4a); (b) mid-range blockers' arrival rate, short blockage duration (Fig. 4b); and (c) high blockers' arrival rate, long blockage duration (Fig. 4c).

In the blockage scenario (a) depicted in Fig. 4a, the MaxMin scheduler (red curve) has the worst performance with respect to PF and BA-PF schedulers. This is because the UEs that suffered from blockage were mostly prioritised even though they had poor channel quality, leading to low user rate. On the contrary, the UEs with better channel quality were less prioritised, also leading to low user rate. Moreover, we observe a smaller discrepancy in performance between PF (blue curve) and BA-PF (yellow, purple and green curves) schedulers. In fact, when there are fewer blockage events, this is expected since the BA-PF priority function in (9) is executed only a few times. In the vast majority of cases, the conventional PF is executed during the prediction window because no blockage is detected.

Furthermore, in the blockage scenario (b) depicted Fig. 4b, where the blockage effect is more severe, the MaxMin

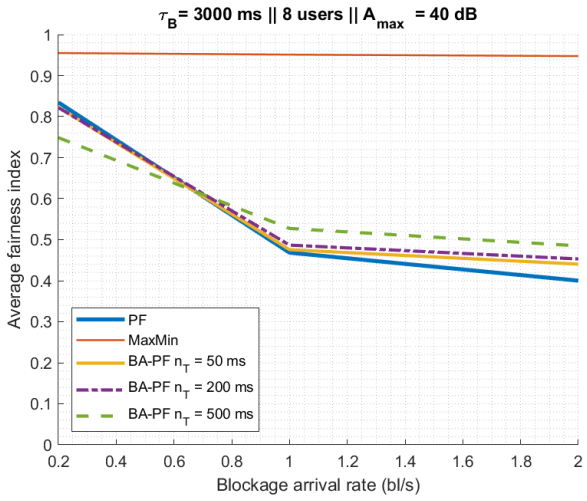

Fig. 5: Average fairness performance as a function of λ_{B}, with $\tau_{\mathrm{B}} = 3000$ ms.

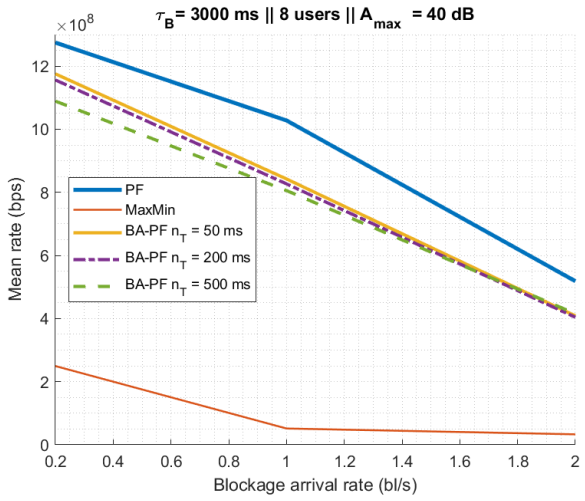

Fig. 6: Mean rate performance as a function of λ_{B}, with $\tau_{\mathrm{B}} = 3000$ ms.

scheduler (red curve) still has the worst performance, while the difference between PF and BA-PF performances increases when looking at the 1st percentile of the ECDF, where we observe a performance gain of 48 % with respect to the PF for all the prediction window values. This is because the BA-PF priority metric in (9) is designed to allocate resources at the beginning of the prediction window and to release them at the end considering that there is only one transition from LOS to NLOS states. Hence, when the blockage duration is short, or there are not as many arrivals as in the blockage scenario (c), multiple state transitions may occur within a large prediction window, leading to a non-ideal scenario for the BA-PF scheduling metric as the resource anticipation is not effective.

Finally, the best performance can be observed for the blockage scenario (c), as depicted in Fig. 4c, when it is more likely that the blockage state is long enough to occur only once within the prediction window. When using the PF scheduler, the UEs that are affected by the blockage are less prioritised as more blockage events occur, decreasing their user rate. Thus, the performance of the PF scheduler (blue curve) approaches the performance of the performance of the MaxMin scheduler (red curve) for the lower values of the ECDF. In contrast, when adopting the BA-PF scheduler, the UEs that suffer from blockage are more prioritised than in the PF scheduler, and we observe gains up to 153 % in the 1st percentile rate with respect to the PF performance for the prediction window value $n_T = 50$ ms (yellow curves). Moreover, this gain is improved to 267 % when increasing the prediction window to $n_T = 500$ ms (green curve in Fig. 4c), as the pool of resources to allocate increase and there is more time to anticipate a transmission for a blocked UE.

C. Network Performance

In Figs. 5 and 6, we show the performance of the network in terms of mean rate and fairness index as a function of the blockage effect. From Fig. 5 we can observe that the MaxMin fairness performance is high (0.95) and is not affected by blockage. The BA-PF performance degrades with λ_{B}, as the blockage scenario gets more severe. This is because the preemptive allocation for UEs suffering from blockage drains a significant amount of resources taken from the pool of all the available resources. Hence, as the blockage severity increases, BA-PF assigns more resources to UEs transitioning to blockage state, disfavouring other UEs, and consequently decreasing fairness. However, the BA-PF fairness is still higher than PF when the blockage arrival rate is high ($\lambda_{\mathrm{B}} \geq 1$ blockers/s), as PF prioritises the allocation of resources to a decreasing number of UEs that are not blocked.

Moreover, from Fig. 6, we can observe that the MaxMin mean rate is significantly lower compared to other schedulers, as the high fairness is achieved by taking away resources from UEs with good channel quality and giving them to UEs with worse quality, levelling down the user rates. We observe that BA-PF and PF mean rates significantly degrade with λ_{B}, as the number of blocked UEs increases. We see that the BA-PF mean rate is up to 22 % lower than the PF mean rate, as the gains achieved by improving the data rate of UEs suffering from blockage comes at the cost of reducing the data rate of non-blocked UEs.

IV. Conclusion

In this work, we assessed the behaviour of schedulers in the event of a blockage affecting the LOS signal path. We showed that the conventional MaxMin scheduler, designed to improve the cell-edge user rate, cannot improve the rate of the users suffering from blockage and has its performance significantly degraded. We showed that the PF scheduler, although it is less affected by blockage compared to MaxMin, can have a user performance as low as MaxMin when blockage scenario is severe. This is because conventional schedulers react to blockage by allocating more resources to compensate the loss in the data rate (as the MaxMin scheduler does), or by allocating fewer resources to prioritise other UEs with better channel conditions (as the PF scheduler does). However, when the UE is entirely in outage, a successful transmission might be impossible to achieve, and any amount of allocated resources may be unused, reducing the efficiency of the allocation.

This reduction in efficiency suggests that conventional schedulers should be adapted to mitigate the blockage effects in the context of 5G-mmWave networks. We therefore considered an adapted scheduling metric BA-PF which relies on blockage prediction to compute the estimated user rates, many slots ahead of a blockage event. The effectiveness of this adaptation is demonstrated by increasing the blockage arrival rate and the blockage duration. We showed that the gain in performance between the BA-PF scheduler and the conventional ones is more significant when the arrival rate and duration are high, i.e., when the channel stays in blockage state long enough to allow for an effective anticipation of resources. This gain is due to an improvement in the rate of users affected by blockage, which is reflected in the gains in the 1st percentile rate and fairness with respect to the PF performance. However, this improvement comes at the expense of performance experienced by other UEs, as reflected on the losses in mean rate performance.

REFERENCES

[1] G. R. Maccartney, T. S. Rappaport, and S. Rangan, "Rapid Fading Due to Human Blockage in Pedestrian Crowds at 5G Millimeter-Wave Frequencies," in *2017 IEEE Global Communications Conference (GLOBECOM)*, Dec. 2017.

[2] R. L. Lella and B. Sikdar, "Blockage Aware Fair Scheduling with Differentiated Service Support in mmWave WPANs/WLANs," *IEEE Transactions on Mobile Computing*, pp. 1–1, July 2019.

[3] M. Alrabeiah and A. Alkhateeb, "Deep Learning for mmWave Beam and Blockage Prediction using Sub-6GHz Channels," *IEEE Transactions on Communications*, June 2020.

[4] Z. Ali, A. Duel-Hallen, and H. Hallen, "Early Warning of mmWave Signal Blockage and AoA Transition Using sub-6 GHz Observations," *IEEE Communications Letters*, pp. 1–1, Nov. 2019.

[5] A. Alkhateeb, I. Beltagy, and S. Alex, "Machine Learning for Reliable mmWave Systems: Blockage Prediction and Proactive Handoff," in *2018 IEEE Global Conference on Signal and Information Processing (GlobalSIP)*, Nov. 2018, pp. 1055–1059.

[6] C. Liu and L. Xiao, "Interference and Blockage Prediction in mmWave-Enabled HetNets," in *2018 IEEE 26th International Symposium on Modeling, Analysis, and Simulation of Computer and Telecommunication Systems (MASCOTS)*, Sep. 2018, pp. 201–208.

[7] T. Nishio, H. Okamoto, K. Nakashima, Y. Koda, K. Yamamoto, M. Morikura, Y. Asai, and R. Miyatake, "Proactive Received Power Prediction Using Machine Learning and Depth Images for mmWave Networks," *IEEE Journal on Selected Areas in Communications*, vol. 37, no. 11, pp. 2413–2427, Nov. 2019.

[8] M. Alrabeiah, A. Hredzak, and A. Alkhateeb, "Millimeter Wave Base Stations with Cameras: Vision Aided Beam and Blockage Prediction," in *2020 IEEE 91st Vehicular Technology Conference (VTC2020-Spring)*, May 2020, pp. 1–5.

[9] H. J. Bang, T. Ekman, and D. Gesbert, "Channel Predictive Proportional Fair Scheduling," *IEEE Transactions on Wireless Communications*, vol. 7, no. 2, pp. 482–487, Feb. 2008.

[10] J. Hajipour and V. C. M. Leung, "Proportional Fair Scheduling in Multi-Carrier Networks Using Channel Predictions," in *2010 IEEE International Conference on Communications*, May 2010, pp. 1–5.

[11] J. F. Schmidt, J. E. Cousseau, R. Wichman, and S. Werner, "Prediction Based Resource Allocation in OFDMA," in *2011 45th Annual Conference on Information Sciences and Systems*, Mar. 2011, pp. 1–4.

[12] R. Margolies, A. Sridharan, V. Aggarwal, R. Jana, N. K. Shankaranarayanan, V. A. Vaishampayan, and G. Zussman, "Exploiting Mobility in Proportional Fair Cellular Scheduling: Measurements and Algorithms," *IEEE/ACM Transactions on Networking*, vol. 24, no. 1, pp. 355–367, Feb. 2016.

[13] L. Shen, T. Wang, and S. Wang, "Proactive Proportional Fair: A Novel Scheduling Algorithm Based on Future Channel Information in OFDMA Systems," in *2019 IEEE/CIC International Conference on Communications in China (ICCC)*, Aug. 2019, pp. 925–930.

[14] A. Noliya and S. Kumar, "Performance Analysis of Resource Scheduling Techniques in Homogeneous and Heterogeneous Small Cell LTE-A Networks," *Wireless Personal Communications*, pp. 1–30, Jan. 2020.

[15] C. Deniz, O. G. Uyan, and V. C. Gungor, "On the Performance of LTE Downlink Scheduling Algorithms: A Case Study on Edge Throughput," *Computer Standards & Interfaces*, vol. 59, pp. 96–108, Aug. 2018.

[16] Y. Wang, Y. Niu, H. Wu, B. Ai, Z. Zhong, D. O. Wu, and T. Juhana, "Relay Assisted Concurrent Scheduling to Overcome Blockage in Full-Duplex Millimeter Wave Small Cells," *IEEE Access*, vol. 7, pp. 105 755–105 767, July 2019.

[17] Y. Niu, W. Ding, H. Wu, Y. Li, X. Chen, B. Ai, and Z. Zhong, "Relay-Assisted and QoS Aware Scheduling to Overcome Blockage in mmWave Backhaul Networks," *IEEE Transactions on Vehicular Technology*, vol. 68, no. 2, pp. 1733–1744, Feb. 2019.

[18] Y. Liu, Q. Hu, and D. M. Blough, "Blockage Avoidance in Relay Paths for Roadside mmWave Backhaul Networks," in *2018 IEEE 29th Annual International Symposium on Personal, Indoor and Mobile Radio Communications (PIMRC)*, Sep. 2018, pp. 1–7.

[19] X. Chen, P. Liu, H. Liu, C. Wu, and Y. Ji, "Multipath Transmission Scheduling in Millimeter Wave Cloud Radio Access Networks," in *2018 IEEE International Conference on Communications (ICC)*, May 2018, pp. 1–6.

[20] W. Chang, C. Wu, and L. Yi-Xin, "Efficient Time-Slot Adjustment and Packet-Scheduling Algorithm for Full-Duplex Multi-Hop Relay-Assisted mmWave Networks," *IEEE Access*, vol. 6, pp. 39 273–39 286, July 2018.

[21] T. K. Vu, C. Liu, M. Bennis, M. Debbah, and M. Latva-aho, "Path Selection and Rate Allocation in Self-Backhauled mmWave Networks," in *2018 IEEE Wireless Communications and Networking Conference (WCNC)*, Apr. 2018, pp. 1–6.

[22] M. Zarifneshat, L. Xiao, and J. Tang, "Learning-Based Blockage Prediction for Robust Links in Dynamic Millimeter Wave Networks," in *2019 16th Annual IEEE International Conference on Sensing, Communication, and Networking (SECON)*, June 2019, pp. 1–9.

[23] Y. Xu, H. S. Ghadikolaei, and C. Fischione, "Adaptive Distributed Association in Time-Variant Millimeter Wave Networks," *IEEE Transactions on Wireless Communications*, vol. 18, no. 1, pp. 459–472, Nov. 2019.

[24] M. Moltafet, R. Joda, N. Mokari, M. R. Sabagh, and M. Zorzi, "Joint Access and Fronthaul Radio Resource Allocation in PD-NOMA-Based 5G Networks Enabling Dual Connectivity and CoMP," *IEEE Transactions on Communications*, vol. 66, no. 12, pp. 6463–6477, Sep. 2018.

[25] M. Gerasimenko, D. Moltchanov, M. Gapeyenko, S. Andreev, and Y. Koucheryavy, "Capacity of Multiconnectivity mmWave Systems With Dynamic Blockage and Directional Antennas," *IEEE Transactions on Vehicular Technology*, vol. 68, no. 4, pp. 3534–3549, Jan. 2019.

[26] M. Polese, M. Giordani, A. Roy, D. Castor, and M. Zorzi, "Distributed Path Selection Strategies for Integrated Access and Backhaul at mmWaves," in *2018 IEEE Global Communications Conference (GLOBECOM)*, Dec. 2018, pp. 1–7.

[27] I. K. Jain, R. Kumar, and S. S. Panwar, "The Impact of Mobile Blockers on Millimeter Wave Cellular Systems," *IEEE Journal on Selected Areas in Communications*, vol. 37, no. 4, pp. 854–868, Apr. 2019.

[28] H. Kim and Y. Han, "A Proportional Fair Scheduling for Multicarrier Transmission Systems," *IEEE Communications Letters*, vol. 9, no. 3, pp. 210–212, Apr. 2005.

[29] E. Liu and K. K. Leung, "Proportional Fair Scheduling: Analytical Insight under Rayleigh Fading Environment," in *2008 IEEE Wireless Communications and Networking Conference*, Mar. 2008, pp. 1883–1888.

[30] A. Duel-Hallen, H. Hallen, and Tung-Sheng Yang, "Long Range Prediction and Reduced Feedback for Mobile Radio Adaptive OFDM Systems," *IEEE Transactions on Wireless Communications*, vol. 5, no. 10, pp. 2723–2733, Oct. 2006.

[31] F. Firyaguna, J. Kibilda, C. Galiotto, and N. Marchetti, "Performance Analysis of Indoor mmWave Networks with Ceiling-Mounted Access Points," *IEEE Transactions on Mobile Computing*, pp. 1–1, Feb. 2020.

[32] S. K. Yoo, S. L. Cotton, R. W. Heath, and Y. J. Chun, "Measurements of the 60 GHz UE to eNB Channel for Small Cell Deployments," *IEEE Wireless Communications Letters*, vol. 6, no. 2, pp. 178–181, Apr. 2017.

[33] S. Ju, O. Kanhere, Y. Xing, and T. S. Rappaport, "A Millimeter-Wave Channel Simulator NYUSIM with Spatial Consistency and Human Blockage," in *2019 IEEE Global Communications Conference (GLOBECOM)*, Dec. 2019, pp. 1–6.

[34] 3GPP 38.211, "NR; Physical Channels and Modulation," 3GPP, Technical Report (TR) V15.1.0, Apr. 2018.

[35] R. K. Jain, D.-M. W. Chiu, and W. R. Hawe, "A Quantitative Measure of Fairness and Discrimination," *Eastern Research Laboratory, Digital Equipment Corporation, Hudson, MA*, Sep. 1984.